

Mu2e Transport Solenoid Prototype Tests Results

M. Lopes, G. Ambrosio, K. Badgley, J. DiMarco, D. Evbota, P. Fabbriatore, S. Farinon, S. Feher, H. Friedsam, A. Galt, S. Hays, J. Hocker, M.J. Kim, L. Kokoska, S. Koshelev, S. Kotelnikov, M. Lamm, A. Makulski, M. Marchevsky, R. Nehring, J. Nogiec, D. Orris, R. Pilipenko, R. Rabehl, C. Santini, C. Sylvester, M. Tartaglia

Abstract— The Fermilab Mu2e experiment has been developed to search for evidence of charged lepton flavor violation through the direct conversion of muons into electrons. The transport solenoid is an s-shaped magnet which guides the muons from the source to the stopping target. It consists of fifty-two superconducting coils arranged in twenty-seven coil modules. A full-size prototype coil module, with all the features of a typical module of the full assembly, was successfully manufactured by a collaboration between INFN-Genoa and Fermilab. The prototype contains two coils that can be powered independently. In order to validate the design, the magnet went through an extensive test campaign. Warm tests included magnetic measurements with a vibrating stretched wire, electrical and dimensional checks. The cold performance was evaluated by a series of power tests as well as temperature dependence and minimum quench energy studies.

Index Terms—Solenoids, Electromagnets, Superconducting magnets.

I. INTRODUCTION

THE Mu2e experiment [1] proposes to measure the ratio of the rate of neutrino-less coherent conversion of muons into electrons in the field of a nucleus, relative to the rate of ordinary muon capture on the nucleus. The conversion process is an example of charged lepton flavor violation, a process that has never been observed experimentally. The conversion of a muon to an electron in the field of a nucleus occurs coherently, resulting in a mono-energetic electron (105 MeV, slightly below the muon rest energy) that recoils from the nucleus.

The Mu2e magnet system can be seen in Fig. 1. It is primarily formed by three large solenoid systems: the Production Solenoid (PS) [2], the Transport Solenoid (TS) [3] and the Detector Solenoid (DS) [4].

A full-scale prototype of a TS coil module was built by a collaboration between Fermilab and INFN-Genoa [5] and is shown schematically in Fig. 2. The coils for this prototype are indicated in Fig. 1 – TS coils 14 and 15. The aluminum housing shell, which contains the two prototype coils, has a square cooling tube for liquid helium welded directly above the coils. The coils are wound from Al-stabilized conductor [6] and surrounded by G10 ground insulation and then impregnated with epoxy resin under vacuum. On the inner surface of each coil is a pure Al sheet. This sheet is connected to the cooling

tube and is used to cool the coil. The coils are inserted in the housing shell by a shrink-fit (SF) procedure. The description of SF for this particular magnet can be seen in [5]. The finished prototype can be seen in Fig. 3.

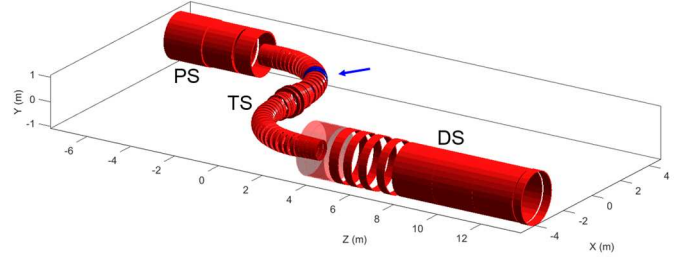


Fig. 1. The Mu2e magnet system – PS, TS and DS. The two coils used in the TS Prototype are highlighted in blue, indicated by arrow.

A test campaign was performed to validate the magnet design choices and to demonstrate that the magnet can be fabricated. This campaign included warm and cold tests.

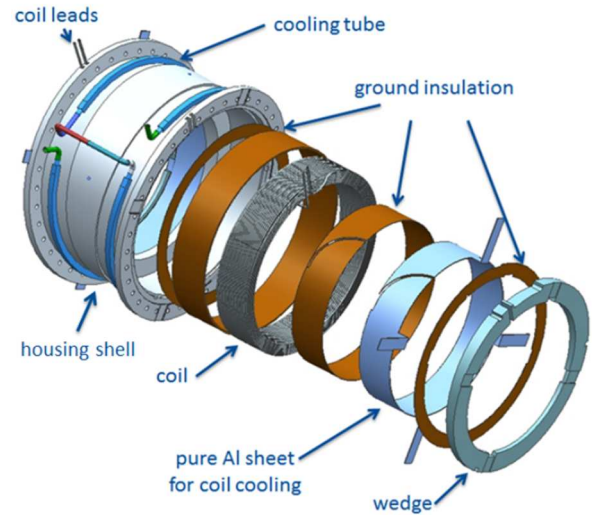


Fig. 2. TS coil module prototype with the main components of one coil pulled apart and out of the module to highlight these components.

II. WARM TESTS

A. Dimensional measurements

The integration of the coils into their housing shell is obtained by a SF operation. In order to guarantee the

appropriate contact between the coil and the shell an interference of $200 \pm 100 \mu\text{m}$ is necessary. More information on the analysis that leads to these numbers as well as a detailed description of the SF operation can be found in [5].



Fig. 3. The TS Prototype on the vibrating stretched-wire station.

In order to verify that the target interference was correctly achieved we measured the outer diameter (OD) of the shell before and after the SF operation using a laser tracker. The results can be found in Table I. Comparing these results with FEA models provides insights into the interference. The measured results are consistent with the desired value for the interference [5].

Alternatively, it was planned to monitor strain gauges to observe the changes in strain before and after the SF. However, due to the temperature applied to expand the shell the sensors were damaged.

TABLE I
MEASUREMENTS OF THE SHELL BEST FIT OD BEFORE AND AFTER THE SF.
TYPICAL MEASUREMENT ERROR IS 50 MICROMETERS

Coil #	Shell OD measurement (mm)	
	Before SF	After SF
14	1030.05	1030.17
15	1029.92	1030.00

B. Electrical test

Using a commercial hipot tester we applied 2000V between the coil and the housing shell. Our acceptance criterion for the leakage current is $10 \mu\text{A}$ or lower. This was done before and after the cold test. Table II presents these results. In both cases, both coils passed the tests showing the choice for the ground insulation was adequate [5].

TABLE II
HIPOT TEST BEFORE AND AFTER THE COLD TESTS WHEN APPLIED 2kV
BETWEEN COIL LEAD AND SUPPORT SHELL

Coil #	Leakage current in (μA)	
	before cold	after cold
	test	test
14	0.2	0.9
15	0.1	0.7

C. Magnetic Measurements

For the transport solenoid, the angular coil orientation during operation - cold and powered - is very important in order to obtain the proper magnetic alignment [7]. In the particular case of the TS prototype, the angle between the two coils has to be $5.5 \pm 0.2^\circ$ at operating conditions.

The angle between the two coils was measured using the vibrating stretched wire technique [8] (Fig. 3). The result for the TS prototype was $5.503(15)^\circ$. The result is significantly better than the requirement, which provides us with the needed level of confidence to validate the features of our mechanical design. Moreover, the relative angles between coils does not change during the cool down.

III. COLD TESTS

A. Test Preparation

A schematic of the TS prototype test stand is shown in Fig. 4. It is the same cryostat used in a previous test [9]. The prototype was supported from the top-hat by four rods connected to brackets. Due to the lack of a liquid nitrogen thermal shield, the magnet is surrounded by pure aluminum ribs that are connected to the return line of the helium ($\sim 10 \text{ K}$) used for the magnet cooling. Thermal anchors were connected to the support brackets and rods as well as the G10 plates that support the magnets leads (not shown in the picture). In order to avoid radiation to the magnet the hardware and the magnet were covered with 40 layers of Multi-Layer Insulation (MLI). This custom thermal shield was very efficient in keeping the magnet cold, however, it was very labor-intensive. Fig. 5 shows the magnet with the custom thermal shield in place.

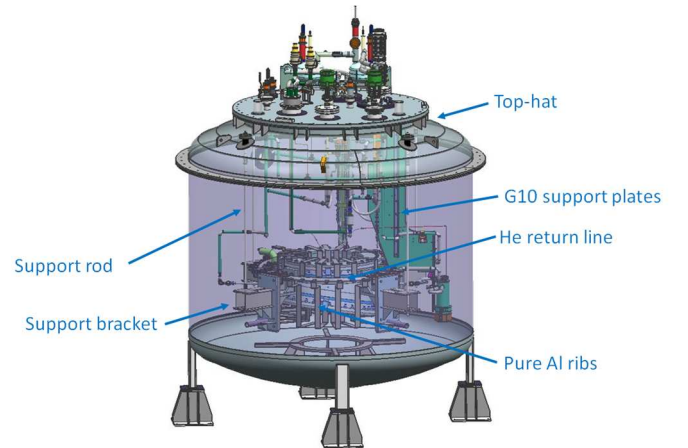


Fig. 4. The TS Prototype in the test stand.

B. Cool down

The temperature of the magnet was monitored at several points in the coil and on the housing shell. The maximum allowable temperature difference was determined by a transient analysis [10] in which the stress between the coil and the housing shell was taken into consideration. The maximum allowed temperature difference (ΔT) was 23 K in the range between room temperature and 70K.



Fig. 5. The prototype with its custom thermal shield finalized and ready to be cold tested.

The cooling-down of the coils from room temperature is essentially done through the housing shell, since the pure Al sheets have poor thermal conductivity at room temperature.

Given the roughness of the coil outer diameter and the SF process, it is very hard to predict the thermal interface between the coil and shell. The most conservative assumption is a large thermal resistance between coil and shell. In this case, keeping below the maximum allowed temperature difference, the cooling rate is about 1 K/h. On the other hand, if one assumes perfect thermal contact in the same interface, the cooling rate would be about 6 K/h for the same ΔT .

Figure 6 shows the cool down of the TS prototype from room temperature until ~ 70 K. As can be seen, the cooling rate was around 4 K/h and it was obtained by constraining the maximum ΔT to 23 K.



Fig. 6. The magnet temperature during cool-down.

C. Power Test

The main test for the validation of the prototype consists of three major tests that can be schematically seen in Fig. 7:

- I. The first test requires that the module hold a test current of up to 2100 A, which is equivalent to 20% over the nominal operating current of 1730 A. At 2100 A the prototype has the same operational margin (with respect to the critical surface) as the full assembled magnet [3, 6].

- II. The second test requires that the module undergo a mechanical stress test in which the current leads of one of the two coils that form the TS prototype module are reversed in polarity such that the forces between the coils will be repulsive. For this part of the test the current will be 1040 A, which is 60% of the operating current and will generate forces comparable to the coil to coil repulsive forces experienced during Mu2e operation.
- III. The current leads has to be restored to their original polarity and the magnet will be once again powered at 2100 A to verify that no changes occurred during the previous step.

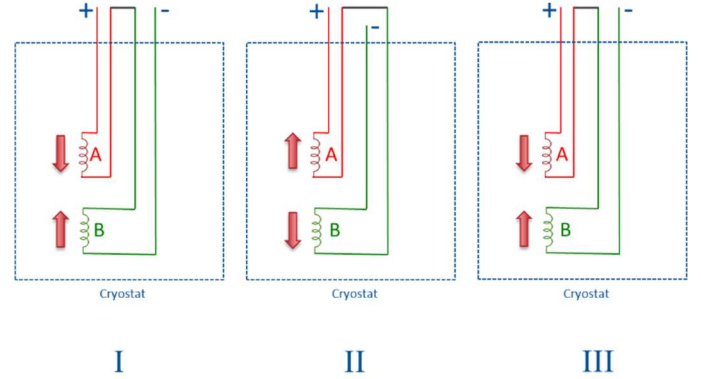


Fig. 7. The TS Prototype main power tests at cold. The arrows indicate the direction of the Lorentz forces acting on the coils.

The initial power test of both coils reached the maximum current of 1896 A before a quench was detected. The thermometers on the coils indicated the temperature was between 5.1 and 5.4 K. After analysis it was identified that the origin of the quench was in lead #3 (coil 14). A second ramp reached 1900 A. Once again a quench originated in lead #3. That coil was disconnected from the power supply and only coil 15 was powered. In that scenario the coil reached 2200 A without any quenches.

The reverse of the leads in one of the coils was performed (step II) and the magnet reached 1040 A without any quenches. Once again we powered both coils in the nominal lead configuration (step III) and once again the magnet reached 1900 A with a quench in lead #3.

The post-test investigation revealed that the problem with lead #3 was a loose screw that did not provide adequate thermal anchoring for the splice between the magnet lead and the HTS lead of the test stand.

D. Temperature Margin Study

In order to study the temperature margin, we connected both coils in series and powered the magnet to its nominal current. The peak field for the prototype at nominal current is 2.2 T. We turned the cooling for the coils off, keeping the leads cold and observed the temperature increasing slowly. The quench happened at 8.0 K – Fig. 8. The prediction was 7.6 K. This result confirms that the operation margin of the TS magnets is around 45% the load line which is consistent with the design target [3].

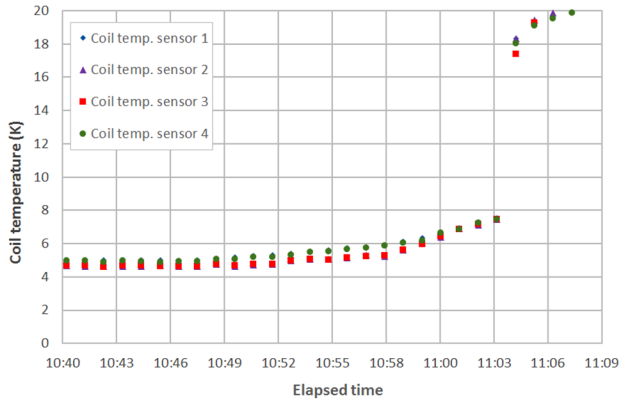


Fig. 8. Magnet temperature as function of time. A quench occurred when the magnet temperature was 8K.

E. Heaters Study

On both coils of this prototype there are four spot heaters located in their inner bores and azimuthally distributed in 90° increments. In addition to the spot heaters built into the coils, two other spot heaters were placed on the housing shell. Fig. 9 shows the locations of these spot heaters.

The heaters on the coils were fired with a 1.5 s flat pulse. Initially a low power pulse was applied and the power was systematically increased until a quench in the coil was initiated. It was required 11 J of energy to induce a quench in the coil. This experiment was repeated using only one heater. And the same result was obtained – 11 J. However, only a fraction of the 11 J is in fact deposited in the coil, since half of the power in the heater is dissipated in the vacuum of the inner bore. Another small fraction of the heater power is taken away by the efficient cooling system of this magnet. These heaters were also used for the verification of quench localization using acoustic emission technique [11].

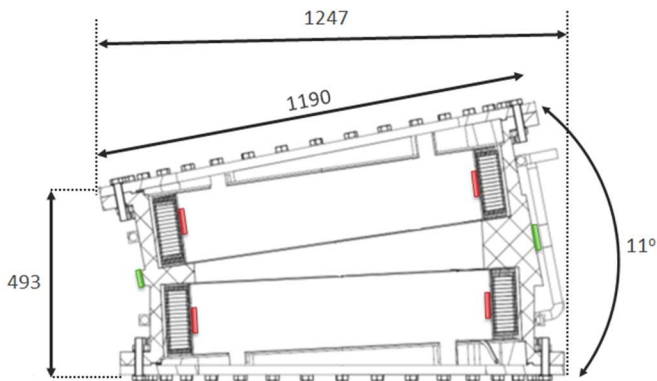


Fig. 9. Cross section of the TS prototype module highlighting the location of the spot heaters on the coils (red) and on the housing shell (green). Dimensions are in mm.

The second test, using the heaters installed on the housing shell, aims to emulate the heat coming from a support rod for the fully assembled Transport Solenoid [3]. The heat coming from supports is estimated to be 1.5 W per rod. We fired each of the heaters with 1.5 W and observed the change of temperature in the coils. There was no noticeable change in temperature in the coils when considering the fluctuation of the measurement system. We then increased the power in each

heater to 2.5 W and then the temperature increase in the coil was about 150 mK. When the heaters were turned off, it took around 10 s for the magnet to cool back down to its original temperature.

F. Strain Gauge Study

Strain Gauges (SG) were installed on the outer diameter of the housing shell, around each coil, 90° apart. The SG were monitored during cool down, coil powering and warm up. The SG were used to determine the change in the pre-stress during cooldown, during powering, and possible changes after thermal and powering cycles. Each gauge was wired to a compensator gauge (for temperature and magnetic field compensation). Each compensator gauge was installed on a thin slab set on the top (in radial the direction) of the reading gauge in order to be exposed to the same magnetic field.

Before the power test described in Section III.C, the magnet went through two thermal cycles: room temperature to 7 K, and room temperature to 5K.

The data analysis showed that during cooldown the coil pre-stress either did not change or increased by a few MPa. The uncertainty is due to differences among the gauges below 50 K, which appear to have been caused by temperature differences between the gauges and their compensators.

During powering cycles the hoop stress in the shell increased as expected up to 2.3 MPa at 2200 A.

The readings at room temperature after two thermal cycles and several powering cycles showed a small loss of pre-stress (~ 3 MPa) [5]. This loss may have been caused by some plastic deformation of the pure aluminum in the conductor during cooldown and powering cycles, as was seen in other solenoids with aluminum stabilized conductors [12]. According to [13] this plastic deformation should reduce and stop during subsequent cycles.

IV. CONCLUSION

The Mu2e Transport Solenoid coil module prototype was successfully tested. The magnet was able to be cooled at the rate of 4 K/h. The magnet was able to be powered using 27% more current than the nominal. When the magnet was powered with the nominal current a quench was initiated at the temperature of 8.0 K. When the current was reversed in one of the coil's leads, no quench due to movement of the coils was registered.

The results shows that the design choices were adequate and the production order of 27 coil modules similar to this prototype can be placed.

REFERENCES

- [1] Mu2e Collaboration, "Mu2e Technical Design Report", arXiv: 1501.05241 <http://arxiv.org/abs/1501.05241>
- [2] V. V. Kashikhin et al., "Conceptual Design of the Mu2e Production Solenoid Cold Mass", *Advances in Cryogenic Engineering*, AIP Conf. Proc., 1434, 2012, p. 893-900.
- [3] G. Ambrosio et al., "Challenges and Design of the Transport Solenoid for the Mu2e Experiment", *IEEE Transactions on Applied Superconductivity* (2014).
- [4] S. Feher et al., "Reference Design of the Mu2e Detector Solenoid", *IEEE Transactions on Applied Superconductivity* (2014).

- [5] P. Fabbriatore et al., “Mu2e Transport Solenoid Prototype Design and Manufacturing”, *this conference*.
- [6] V. Lombardo, “Aluminum Stabilized Superconducting Prototype Cable Development for the Mu2e Transport Solenoid”, IEEE Transactions on Applied Superconductivity (2015).
- [7] M. Lopes et al., “Studies on the magnetic center of the Mu2e solenoid system”, IEEE Transactions on Applied Superconductivity (2014).
- [8] J. DiMarco et al., “Certification of Superconducting Solenoid-Based Focusing Lenses” - IEEE Transactions on Applied Superconductivity (2011).
- [9] R. Rabehl et al., “A Cryogenic Test Stand for Large Superconducting Solenoid Magnets”, IEEE Transactions on Applied Superconductivity (2015).
- [10] N. Dhanaraj and E. Voirin, “TS Cool Down Studies TSu Unit Coils”, Mu2e Internal Document:
<http://mu2e-docdb.fnal.gov/cgi-bin/ShowDocument?docid=6097>
- [11] M. Marchevsky et al., “Localization of Quenches and Mechanical Disturbances in the Mu2e Prototype Solenoid Using Acoustic Emission Technique”, *this conference*.
- [12] R. Musenich, et al. “Results From the Testing of the AMS Space Superconducting Magnet”, IEEE Transactions on Applied Superconductivity (2012).
- [13] K.T. Hartwig, et al. “The effect of low temperature fatigue on the RRR and strength of pure aluminum” IEEE Transactions on Magnetics, Vol. MAG-21, No. 2, pp. 161-164 (1985).